SEMARAK ILMU PUBLISHING

Journal of Advanced Research in Fluid Mechanics and Thermal Sciences

Journal homepage:
https://semarakilmu.com.my/journals/index.php/fluid_mechanics_thermal_sciences/index
ISSN: 2289-7879

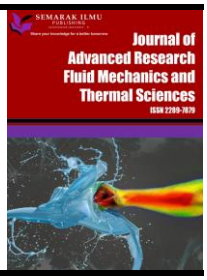

Design of Open Flume Turbine using Specific Speed of Power and Discharge

Warjito[1], Kevin Kameswara[1], Budiarso[1], Muhamad Mizan[1,*], Sanjaya Baroar Sakti Nasution[1], Muhammad Agil Fadhel Kurnianto[1], Christopher Clement Rusli[2]

[1] Department of Mechanical Engineering, University of Indonesia, Depok, Indonesia
[2] Department of Mechanical Engineering, University of Malaya, Kuala Lumpur, Malaysia

ARTICLE INFO

Article history:
Received 3 May 2024
Received in revised form 11 September 2024
Accepted 20 September 2024
Available online 10 October 2024

Keywords:
Open flume; Pico-hydro; specific speed; electrification

ABSTRACT

Open flume turbine is a pico-hydro water turbine that can generate electricity up to 5 kW with low head. The open flume turbine typically designed using power specific speed, however Simpson proposed a method using discharge specific speed for pico-propeller turbine. This study compares the performance of pico-hydro open flume turbines designed with power specific speed and flow specific speed. The turbines are designed with 2.71m head with various flowrates. The flowrates are chosen so that the flow specific speeds are 140, 160, 180, and 200. Based on the result, the turbines designed using flow specific speed yield higher power output and efficiency at all designed flowrates.

1. Introduction

Indonesia is the fourth most populated country in the world, with a total population of 276 million people [1]. However, around 1% of the population has not yet to receive electricity, with most of them located in rural areas on the eastern side of Indonesia [2]. One of the main reasons for this is due to the high cost of setting up the electrical grid system in those areas [3]. This problem can be solved with off-grid electrification since it eliminates the need to construct the infrastructure needed to provide on-grid electrification.

There are several types of power plant which could provide off-grid electrification such as water turbines, wind turbines, biomasses, and solar photovoltaics. As a tropical country located near the equator, the highest off grid potential in Indonesia is solar energy with 207.8GWp followed by water energy with 94.3GW power [4]. Depending on the site, hydropower could give a lower cost and a more stable power supply compared to photovoltaics since the latter is heavily dependent on weather [5]. Indonesia also has an area that is mainly filled with water. The provision of energy access in Indonesia is also related to the quality of electricity received by the community [6].

* *Corresponding author.*
E-mail address: muhammadmizan3012@gmail.com

https://doi.org/10.37934/arfmts.122.1.5668

A Pico-hydro turbine is a water turbine with a power rating below 5kW. A Pico hydro turbine can be an alternative to rural electrification in Indonesia due to its lower cost of manufacture and maintenance. For rivers with low head, a reaction turbine is usually preferred due to having higher efficiency on low head [7]. An Open-flume Francis turbines; head from 1.5m up to 10m and is a fixed-blade propeller turbine with open spiral casing [8,9]. Compared to Kaplan turbine, open flume turbines have lower costs on both manufacture and maintenance, hence open flume turbine is preferred when it comes to rural electrification [10]. In addition, open flume turbine safe for the fish through it [11].

Several studies have been made regarding open flume turbines. Nasution and Adanta [9] studied the effect of tangential absolute velocity at the outlet on open flume turbine performance and found that tangential velocity based on Nechleba's method to yield better result compared to tangential velocity based on Euler's method. Warjito *et al.,* [12] compared plate and airfoil blade performance in open-flume turbines and found that plate blades are more suitable for open flume turbine compared to airfoil blade. Adanta *et al.,* [13] investigated the effect of gaps between the blades of open flumes turbine and found that larger gaps increase losses. Vu *et al.,* [14] proposed a design of pico-hydro propeller turbine for water supply networks in urban areas. Simpson and Williams [15] studied the application of computational fluid dynamics to the design of pico-hydro propeller turbines.

One of the parameters determined in the turbine design is the runner diameter and number of blades. Turbine diameter is usually determined using power specific speed [16]. However, Simpson and Williams [15] proposed a method using a discharge specific speed in determining the diameter of pico-propeller turbine. Nasution *et al.,* [17] compared open flume turbine design with specific needs based on power and discharge function and found that design with specific needs based on power to have better performance. However, the study is limited to water flowrate of 0.041m^3/s. On this study, the analysis is done to various flowrates to analyze the effect of different flowrates to the efficiency of turbines designed with both methods. The limitation of this study using a head of 2.7 m, the acceleration of gravity is 9.81 m/s^2, water temperature and ambient air.

2. Methodology

2.1 Specific Speed

In this study, eight runners are designed for four specifications and divided into groups of two. Group A is comprised of turbines designed with power specific speed method proposed by Nechleba [16] and Group B is comprised of turbines designed with discharge specific speed method proposed by Simpson and Williams [15]. The power specific speed and the discharge specific speed used in this study are defined with the Eq. (1) and Eq. (2) respectively.

$$n_p = \frac{\chi^{1/2}}{\psi^{5/4}} = \frac{N\sqrt{P}}{H^{5/4}} \tag{1}$$

$$n_q = \frac{\phi^{1/2}}{\psi^{3/4}} = \frac{N\sqrt{Q}}{H^{3/4}} \tag{2}$$

The head is set to 2.7 m and the angular velocity is set to 1400 rpm. The discharge specific speed, flowrates and power specific speed is in Table 1. Variation of discharge specific speeds are 140, 160, 180, and 200.

Table 1
Discharge specific speed, flowrate, and power specific speed of the turbines

n_q	$Q(m^3/s)$	P(kW)	n_p
140	0.044	1.174	438.4
160	0.057	1.534	501.0
180	0.073	1.941	563.7
200	0.090	2.397	626.3

To determine the diameter and number of blades, the turbines in Group A uses Table 2. The table determines the number of blades and the diameter ratio based on power specific speed. Blade height with low hub-tip ratio is relatively longer, and the aerodynamic parameters change drastically from hub to tip [17].

Table 2
Determining hub to tip ratio and number of blades using power specific speed

Specific Speed about	1000	800	600	400	350	300
Hub to tip ratio	0.3	0.4	0.5	0.55	0.6	0.7
Number of Blades	3	4	5	6	8	10

The tip diameter is then determined by calculating the value of C_x by using Eq. (3). The Value of C_x is calculated by using cm which can be determined using Figure 1.

$$\boldsymbol{D = \sqrt{\frac{4Q}{\pi C_x\left(1-\left(\frac{d_h}{D}\right)^2\right)}}} \tag{3}$$

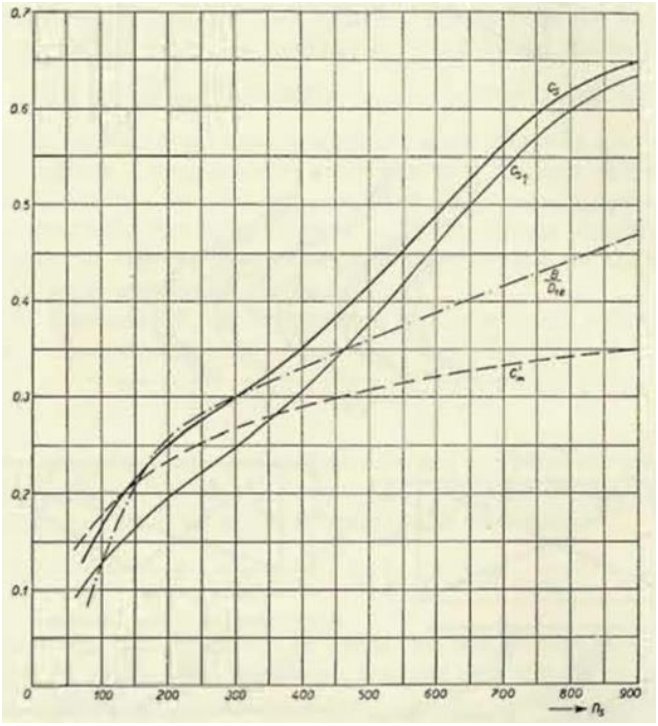

Fig. 1. Determining c_m using power specific speed [16]

To determine hub-to-rip ratio and number of blades in Group B, discharge specific speed was used. Using Figure 2, the number of blades, kug and hub-to-tip ratio can be determined using discharge specific speed.

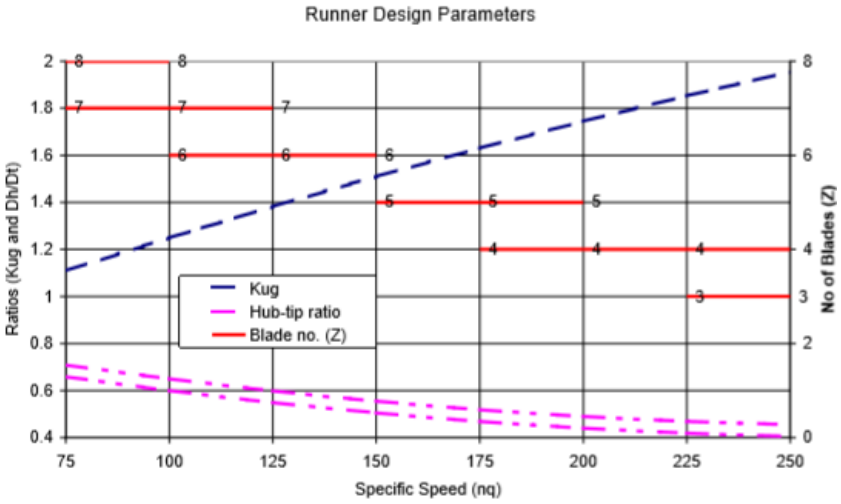

Fig. 2. Determining hub-to-tip ratio, blade number, and Kug using discharge specific speed

The tip diameter is then determined using Eq. (4) with the corresponding value of kug from Figure 2.

$$Kug = \frac{r_{tip} * \omega}{\sqrt{2gH}} \tag{4}$$

The blade profiles are determined by using velocity triangle from Figure 3, there is absolute velocity (C), relative inlet velocity (w_1) which results in the angle of entry (β_1) and relative velocity in which results in the angle of exit (β_2), $\boldsymbol{\alpha}$ for angle of attack, U for tangential velocity, $C_{x\ is}$ velocity against tangential, C_r is radial velocity. For both methods, Necleba's recommendation for velocity triangle used [16].

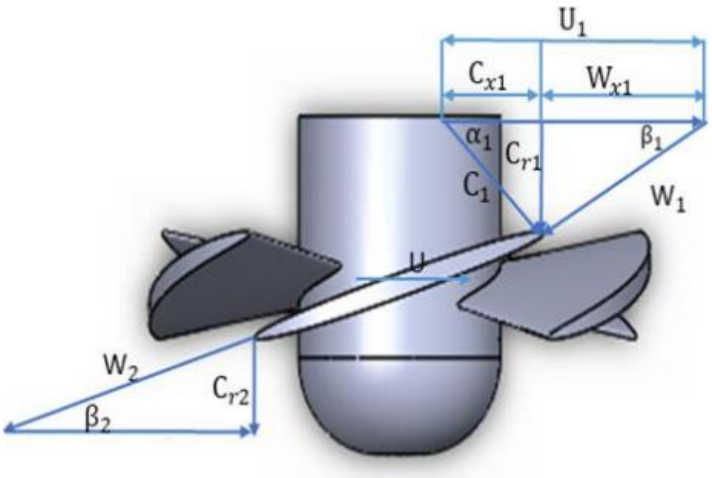

Fig. 3. The blade profile is designed using velocity triangle

The velocity triangle in Figure 1 could be described with these equations:

$$\boldsymbol{C = U + W} \tag{5}$$

$$\boldsymbol{C = C_x + C_r} \tag{6}$$

$$\boldsymbol{C_r = W + W_x} \tag{7}$$

Eq. (7) is based on Nechleba's recommendation [16]. From hub to tip, the runner blades are divided into three sections. Since each section of the blades yields different velocity triangles, the airfoil and blade angle of each section are different from those of different sections. The velocity triangle calculations were then calculated for those three sections.

ANSYS Fluent 18.1 was used to perform CFD analysis on the runners. Three-dimensional (3D) analysis is used in this study as seen Figure 4. Inlet was set as a mass flow boundary inlet with the values corresponding to the flowrate at Table 1. The outlet was defined as a pressure outlet with a gauge pressure of 1 Pa. The steady flow model was used. The torque and power output from Group A and Group B would then be compared. The turbulent model to be used is the k-epsilon model. Nasution *et al.* used the k-epsilon model to predict the working of the propeller turbine blades and the resulting error of 10% [9]. The K-Epsilon model can reduce computing power for turbo engine cases [9]. The simulation was carried out using three-dimensional geometry using the Multiple Reference Frame (MRF) method. The governing equations were resolved using the SIMPLE scheme for pressure-velocity coupling. The solution was discretized spatially through a cell-based least squares gradient approach, along with a first-order upwind method for momentum, turbulent kinetic energy, and turbulent dissipation rate [18]. In this method, the rotational speed is determined according to the design and the torque received by the blades will be processed to obtain power. The inlet is set to a mass-flow inlet with a large mass-flow according to the water discharge of the design of each blade described in Table 3.

Table 3
Boundary Condition for Simpson dan Nechleba blade

Nsq	Massflow inlet (kg/s)	Outlet	Blade
140	44.36	Pressure Outlet 1 atm	Rotor & Stator Interface
160	57.95	Pressure Outlet 1 atm	Rotor & Stator Interface
180	73.34	Pressure Outlet 1 atm	Rotor & Stator Interface
200	90.54	Pressure Outlet 1 atm	Rotor & Stator Interface

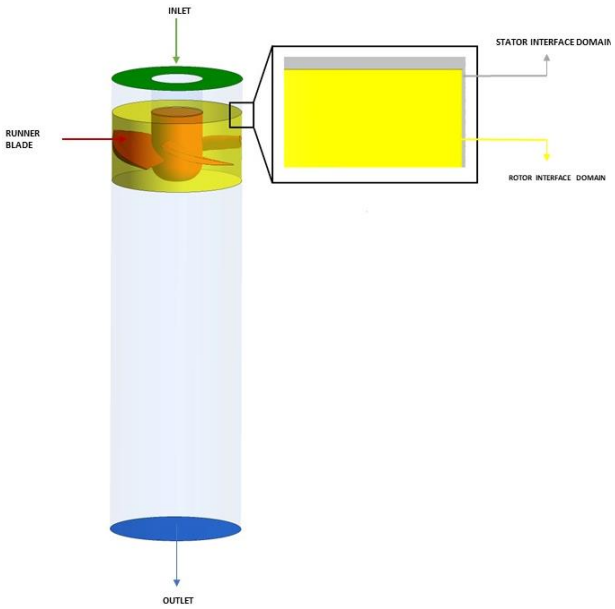

Fig. 4. Boundary Condition for simulation

Mesh Independency test was conducted. The Grid Convergence Index (GCI) and Least Squares (LS) procedures were employed to estimate discretization error and associated uncertainties [19]. The Grid Convergence Index method requires at least three systematic mesh refinements, each requiring the numerical solution to be in the asymptotic range [20]. The mesh sizes are divided into fine, medium, and coarse for each classification. The tests were done in a steady, non-rotational setting. The torques of each mesh size were then obtained. GCI test was then performed to determine the error percentage of mesh pairings: coarse-to-medium and medium-to-fine. GCI for medium-to-fine was then obtained using equations below. The computational time for medium mesh was acceptable for simulation, and it will not vary substantially even if the grid is refined further [21].

$$GCI_{fine}^{21} = \frac{1.25e_a^{21}}{r_{21}^p - 1} \tag{7}$$

$$e_a^{21} = \frac{|T_1 - T_2|}{T_1} \tag{8}$$

$$p = |\ln\left|\frac{\varepsilon_{32}}{\varepsilon_{21}}\right| + \ln\left(\frac{r_{21}^p - s}{r_{32}^p - s}\right) \tag{9}$$

$$s = \text{sgn}\left(\frac{\varepsilon_{32}}{\varepsilon_{21}}\right) \tag{10}$$

In this case the Grid Independency Test is performed by comparing three types of grids: coarse, medium, and fine for each specific speed using the Grid Convergence Method (GCI). Here is Table 4 for GCI calculation results for the four specific speed types to be simulated.

Table 4
GCI calculation for Nechleba and Simpson Blade simulation

Ns	Grid 1	Grid 2	Grid 3	GCI21	GCI32
140	2571207	1642526	1183931	0.01943	0.08183
160	2969447	1929262	1401560	0.003035	0.037372
180	3225233	2084567	1526642	0.030157	0.008007
200	3644191	2433794	1803465	0.180908	0.324982

Figure 5 give the information about the blade is divided into three sections. A velocity triangle is then calculated for each section. The geometry on each section were then created based on the velocity triangles. The geometry details, the difference in NACA in each section is different because the blade shape of the open flume forms a chamber line that is not straight because the angle of entry and exit of the turbine blades is different and the calculation method of Nechleba and Simpson is different are presented in Table 5 to Table 12.

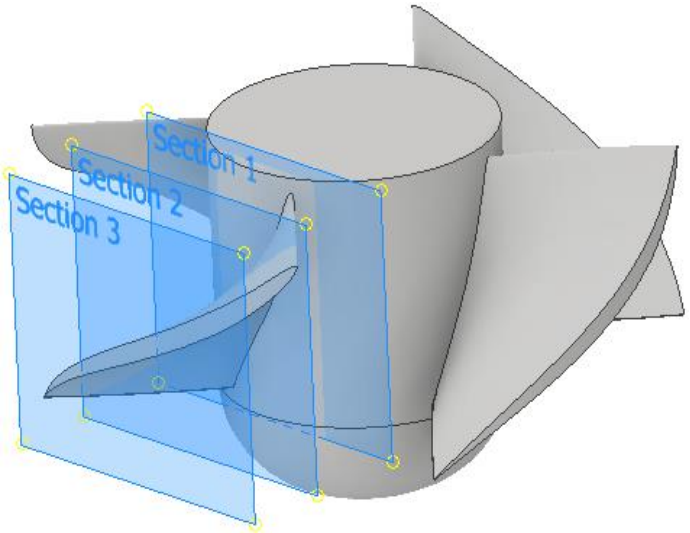

Fig. 5. Three sections of the blade

Table 5
Blade Geometry of Simpson Model nq 140

Section	Radial Coordinate (mm)	Beta 1 (deg)	Beta 2 (deg)	Stagger angle (deg)	Cord length (mm)	NACA airfoil
1	39.78	54.87	68.45	61.66	45.93	6513
2	55.34	63.17	70.19	66.68	63.90	3509
3	70.89	68.46	72.42	70.44	81.86	1507

Table 6
Blade Geometry of Simpson Model nq 160

Section	Radial Coordinate (mm)	Beta 1 (deg)	Beta 2 (deg)	Stagger angle (deg)	Cord length (mm)	NACA airfoil
1	40.49	53.03	66.78	59.90	58.84	6510
2	58.23	62.37	69.01	65.69	84.61	3507
3	75.96	68.13	71.71	69.92	110.37	1505

Table 7
Blade Geometry of Simpson Model nq 180

Section	Radial Coordinate (mm)	Beta 1 (deg)	Beta 2 (deg)	Stagger angle (deg)	Cord length (mm)	NACA airfoil
1	40.92	51.47	65.39	58.43	59.46	6510
2	60.97	61.88	68.15	65.01	88.60	3506
3	81.02	68.09	71.30	69.70	117.73	1505

Table 8
Blade Geometry of Simpson Model nq 200

Section	Radial Coordinate (mm)	Beta 1 (deg)	Beta 2 (deg)	Stagger angle (deg)	Cord length (mm)	NACA airfoil
1	41.07	50.08	64.23	57.16	82.14	6507
2	63.5	61.61	67.52	64.56	127.16	2505
3	86.08	68.24	71.12	69.67	172.17	1504

Table 9
Blade Geometry of Nechleba Model nq 140 (np 438.4)

Section	Radial Coordinate (mm)	Beta 1 (deg)	Beta 2 (deg)	Stagger angle (deg)	Cord length (mm)	NACA airfoil
1	53.88	75.04	79.38	77.21	62.22	1509
2	75.92	79.26	81.12	80.19	87.67	1507
3	97.97	81.64	82.58	82.11	113.12	0505

Table 10
Blade Geometry of Nechleba Model nq 160 (np 501)

Section	Radial Coordinate (mm)	Beta 1 (deg)	Beta 2 (deg)	Stagger angle (deg)	Cord length (mm)	NACA airfoil
1	60.04	75.82	79.36	77.60	69.34	1508
2	84.61	79.85	81.32	80.59	97.70	1506
3	109.18	82.10	82.83	82.47	126.07	0505

Table 11
Blade Geometry of Nechleba Model nq 180 (np 563.7)

Section	Radial Coordinate (mm)	Beta 1 (deg)	Beta 2 (deg)	Stagger angle (deg)	Cord length (mm)	NACA airfoil
1	57.37	74.29	78.44	76.37	83.36	1507
2	86.06	79.38	80.87	80.13	125.05	1505
3	114.74	81.98	82.67	82.33	166.73	0504

Table 12
Blade Geometry of Nechleba nq 200 (np 626.3)

Section	Radial Coordinate (mm)	Beta 1 (deg)	Beta 2 (deg)	Stagger angle (deg)	Cord length (mm)	NACA airfoil
1	63.26	75.48	78.81	77.147	91.92	1506
2	94.89	80.20	81.37	80.78	137.83	1504
3	126.56	82.62	83.14	82.88	183.85	0503

3. Results and Discussions

Figure 6 and Figure 7 show the comparison of power and hydraulic efficiency produced by both turbines. It shows that the power peaks at discharge specific speed of around 180 and the efficiency peaks at discharge specific speed of around 150. Turbines designed using Simpson's method has higher power output and efficiency. A study using Simpson's method by Adhikari [22] results in efficiency of 53.8% which is like the efficiency produced by Simpson 140 in this study.

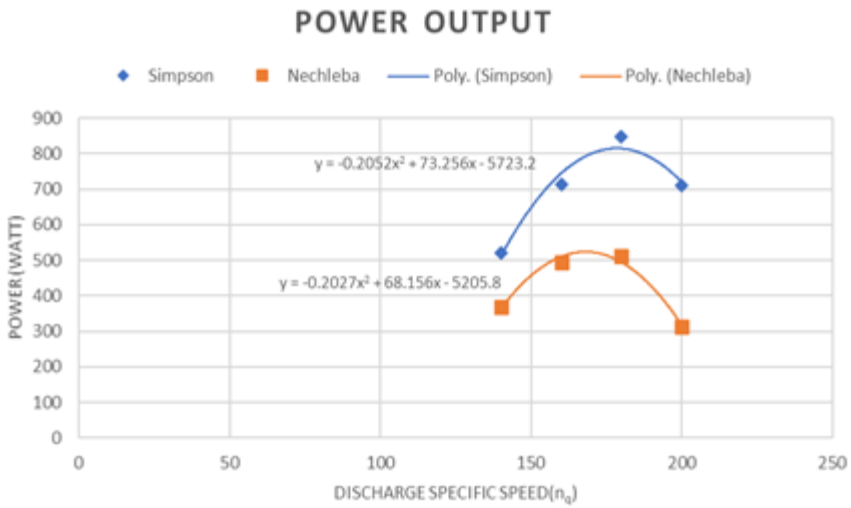

Fig. 6. Power output comparison

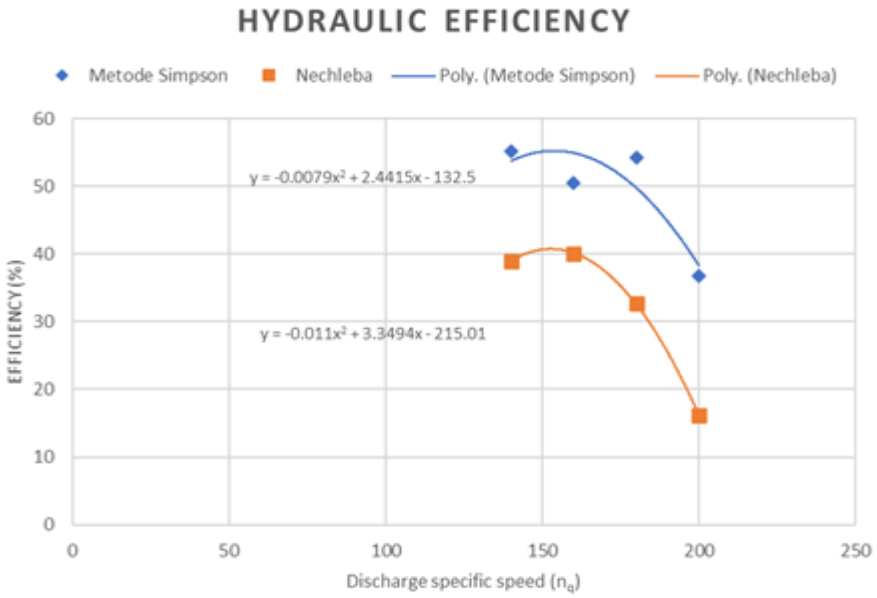

Fig. 7. Efficiency comparison

The midspan (section 2) of the blades is used for pressure contour. It can be seen from Figure 8 that the turbines designed using Simpson's method has higher pressure difference between the suction and the pressure side. This is mainly because the turbines designed using Simpson method has higher camber compared to the turbines designed using Nechleba's method. The higher-pressure difference causes higher lift, which causes the turbines designed using Simpson's method to yield more torque, and hence more power. This can be explained using Euler's turbomachinery equation. It dictates that higher camber results in higher turns of the streamline, which causes higher difference in radial velocity of the near upstream and downstream. The higher difference will then result in higher hydraulic power.

Discharge Specific Speed	Simpson	Nechleba
140	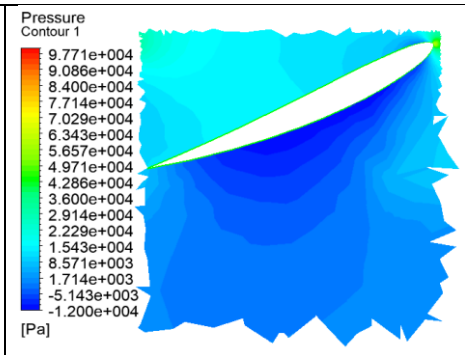	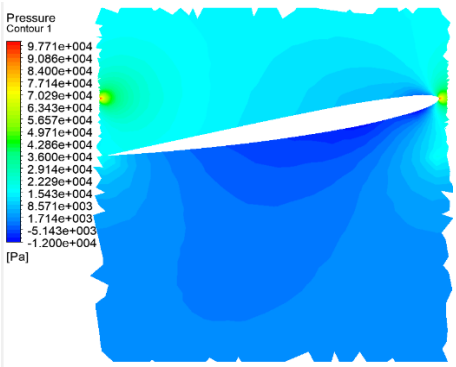
160	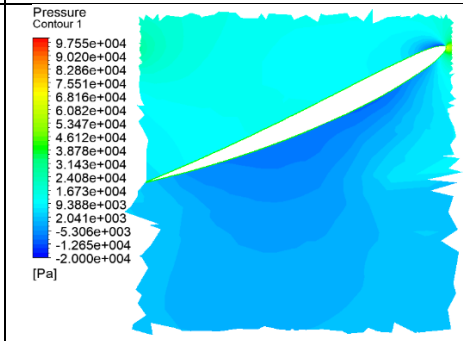	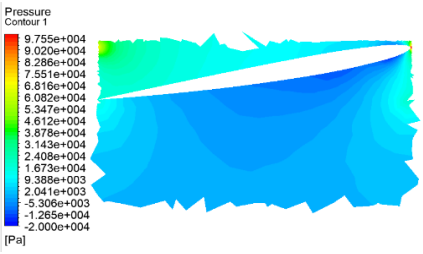
180	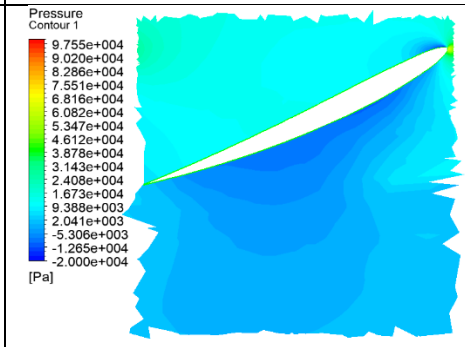	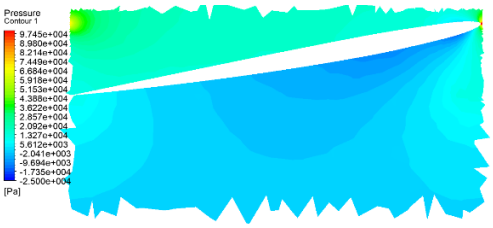
200	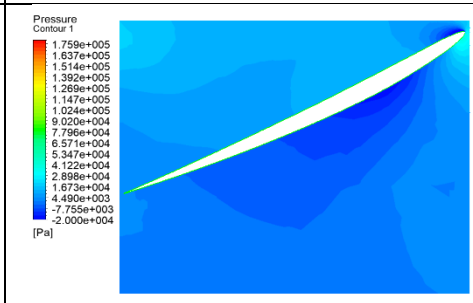	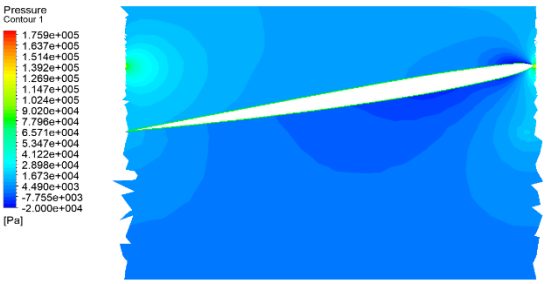

Fig. 8. Pressure countour in midspan

Figure 9 shows the velocity streamline for both types of blades at a specific discharge velocity of 140. From the figure, it can be seen that both types of blades have an angle of attack that is close to zero. This is due to the speed triangle design that makes the blades have a direction that is in accordance with the streamline so as to reduce losses. In the figure, it can be seen that the Simpson blade deflects the velocity vector greater than the Nechleba blade. This causes a greater lift force, resulting in greater power. This is in accordance with Euler's turbomachinery equation which explains the relationship between the speed triangle and the resulting power.

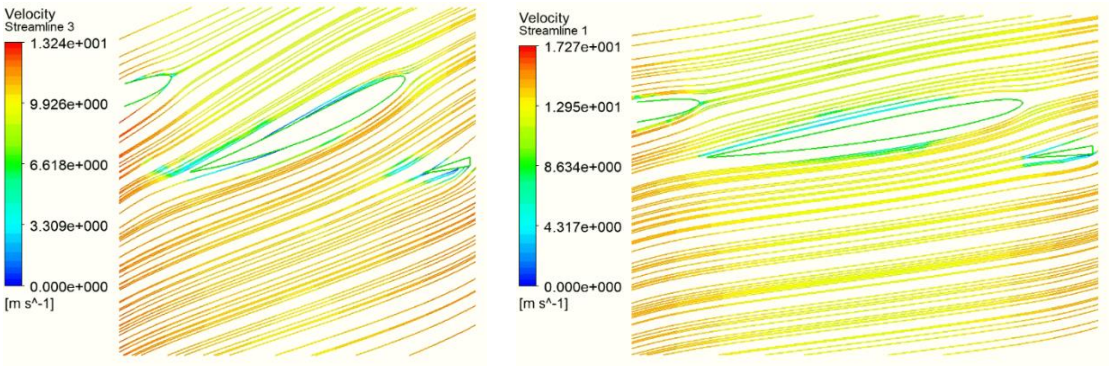

(a) (b)

Fig. 9. Velocity Streamline. (a) Simpson n_q 140 (b) Nechleba n_q 140. Simpson's turbine shows higher turns which results in higher tangential velocity difference

This result is not in line with the previous study, which shows that design using Nechleba yields a better result [23]. The difference in result is suspected to be caused by the lower discharge specific speed used by the previous study. To confirm this, a simulation was done using the specification of nq 140 but with doubled head and halved discharge, which resulted in n_q 59. The velocity streamline Simpson There is a high velocity at the bottom of the airfoil of 13.24 m/s causing a higher pressure compared to Nechleba of 8.63 m/s can be seen in Figure 9.

The result shows that turbines designed with Nechleba's method yield better results. This is caused by a change of blade geometry at lower specific speed. At lower speed, Nechleba's turbine blades have higher camber which results in higher lift and higher torque. To further analyze the relation between specific speed and the result, further analysis was done by varying the discharge of the two new turbines above to create turbines with specific speeds of 80 and 100. The efficiency of the entire result is presented in Figure 7.

The result in Figure 10 shows that Nechleba's turbine yields better results at lower specific speed, with the threshold discharge specific speed of around 130. The previous study's result is shown at discharge specific speed of 114. This is caused by the geometry changes that happen at lower specific speed, as previously discussed. These results mean that the Nechleba's method is more suitable for open flume pico hydro turbine with lower specific speed and the Simpson's method is more suitable for the higher specific speed.

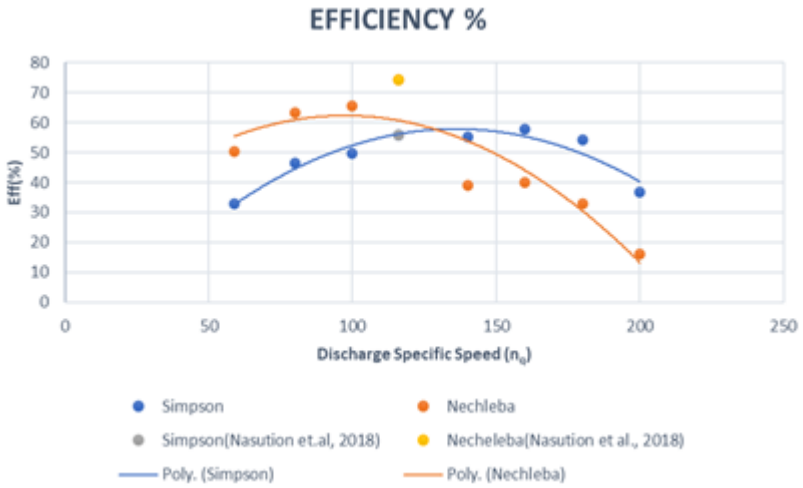

Fig. 10. Efficiency comparison; the result of the previous study is shown in yellow (Nechleba) and grey (Simpson)

4. Conclusion

This study analyses the performance of open flume pico hydro turbines designed with Simpson's method and Nechleba's method. Simpson's method uses discharge specific speed to determine turbine diameter and number of blades, while Nechleba's method uses power specific speed. The turbines are made in different specification based on the specific speed. The result shows that Simpson's turbines yield better result at higher specific speed while Nechleba's turbines yield better result at lower specific speed.

Acknowledgement

This work was supported by PUTI Universitas Indonesia with grant no: NKB-286/UN2.RST/HKP.05.00/2023.

References

[1] BPS. "Statistical Yearbook of Indonesia 2021." *BPS-Statistics Indonesia*, 2021.
[2] Kementerian Energi Dan Sumber Daya Mineral Republik Indonesia. "Capaian Kerja 2019 Dan Program 2020." *Kementerian Energi Dan Sumber Daya Mineral Republik Indonesia*, 2020.
[3] Brata, Teguh Jiwa. "Menurut PLN, ini penyebab elektrifikasi wilayah Indonesia Timur rendah." *JawaPos*. March 8, 2018.
[4] Kementrian Energi dan Sumber Daya Mineral Republik Indonesia. "Indonesia Energy Outlook 2020." *Kementrian Energi dan Sumber Daya Mineral Republik Indonesia*, 2019.
[5] Maher, P., N. P. A. Smith, and A. A. Williams. "Assessment of pico hydro as an option for off-grid electrification in Kenya." *Renewable Energy* 28, no. 9 (2003): 1357-1369. https://doi.org/10.1016/S0960-1481(02)00216-1
[6] Mizan, Muhammad, Warjito Warjito, Budiarso Budiarso, Ridho Irwansyah, Muhamad Agil Fadhel Kurnianto, and Muhammad Faridz Athaya. "The performance of the pico scale turgo water turbine coconut shell blade with variations in nozzle diameter and distance." *Journal of Advanced Research in Fluid Mechanics and Thermal Sciences* 100, no. 1 (2022): 53-62. https://doi.org/10.37934/arfmts.100.1.5362
[7] Kothandaraman, C. P., and R. Rudramoorthy. *Fluid mechanics and machinery*. New Age International, 2007.
[8] Vijay Kumar, Megavath, T. Subba Reddy, P. Sarala, P. Srinivasa Varma, Obbu Chandra Sekhar, Abdulrahman Babqi, Yasser Alharbi, Basem Alamri, and Ch Rami Reddy. "Experimental investigation and performance characteristics of Francis turbine with different guide vane openings in hydro distributed generation power plants." *Energies* 15, no. 18 (2022): 6798. https://doi.org/10.3390/en15186798
[9] Nasution, Sanjaya B. S., and Dendy Adanta. "Effect of tangential absolute velocity at outlet on open flume turbine performance." In *IOP Conference Series: Earth and Environmental Science*, vol. 431, no. 1, p. 012023. IOP Publishing, 2020. https://doi.org/10.1088/1755-1315/431/1/012023
[10] Rao, N. S. Govinda. *Fluid Flow Machines*. Tata McGraw-Hill, 1983.
[11] Li, Minne, Ruidong An, Min Chen, and Jia Li. "Evaluation of volitional swimming behavior of Schizothorax prenanti using an open-channel flume with spatially heterogeneous turbulent flow." *Animals* 12, no. 6 (2022): 752. https://doi.org/10.3390/ani12060752
[12] Warjito, Warjito, Sanjaya Nasution, Dendy Adanta, Budiarso Budiarso, and Ahmad Indra Siswantara. "Comparison of plate and aerofoil blade performance in open-flume turbines." In *AIP Conference Proceedings*, vol. 2227, no. 1. AIP Publishing, 2020. https://doi.org/10.1063/5.0001620
[13] Adanta, Dendy, Emanuele Quaranta, and T. M. I. Mahlia. "Investigation of the effect of gaps between the blades of open flume Pico hydro turbine runners." *Journal of Mechanical Engineering and Sciences* 13, no. 3 (2019): 5493-5512. https://doi.org/10.15282/jmes.13.3.2019.18.0444
[14] Vu, Viet Luyen, Zhenmu Chen, and Young-Do Choi. "Effect of the Hub to Tip Diameter Ratio to the Performance of a Bulb Hydro Turbine Model." *The KSFM Journal of Fluid Machinery* 22, no. 3 (2019): 5-11. https://doi.org/10.5293/kfma.2019.22.3.005
[15] Simpson, R. G., and A. A. Williams. "Application of computational fluid dynamics to the design of pico propeller turbines." In *Proceedings of the International Conference on Renewable Energy for Developing Countries*, pp. 5-7. University of the District of Columbia Washington, DC, 2006.
[16] Nechleba, Miroslav. *Hydraulic turbines: their design and equipment*. Artia, 1957.

[17] Nasution, Sanjaya Baroar Sakti, Warjito Warjito, Budiarso Budiarso, and Dendy Adanta. "A Comparison of Openflume Turbine Designs with Specific Speeds (Ns) Based on Power and Discharge Function." *Journal of Advanced Research in Fluid Mechanics and Thermal Sciences* 51, no. 1 (2018): 53-60.

[18] Sari, Dewi Puspita, Dendy Adanta, Imam Syofii, Wadirin Wadirin, Aji Putro Prakoso, Dadan Hermawan, Ahmed Al-Manea, Ramiz Ibraheem Saeed, Ahmad Fudholi, and Subagyo Subagyo. "Feasibility Study of Small-Diameter Pico-Hydro Breastshot Waterwheel by Computational Method." *CFD Letters* 15, no. 11 (2023): 169-180. https://doi.org/10.37934/cfdl.15.11.169180

[19] Nandi, Tarak N., and DongHun Yeo. "A Solution Verification Study for URANS Simulations of Flow Over a 5: 1 Rectangular Cylinder Using Grid Convergence Index and Least Squares Procedures." *Journal of Verification* 8 (2023): 041001-1. https://doi.org/10.1115/1.4063818

[20] Baker, Nazar, Ger Kelly, and Paul D. O'Sullivan. "A grid convergence index study of mesh style effect on the accuracy of the numerical results for an indoor airflow profile." *International Journal of Ventilation* 19, no. 4 (2020): 300-314. https://doi.org/10.1080/14733315.2019.1667558

[21] Mohd Zainuddin, Nor Azira, Fauziah Jerai, Azli Abd Razak, and Mohd Faizal Mohamad. "Accuracy of CFD simulations on indoor air ventilation: application of grid convergence index on underfloor air distribution (UFAD) system design." *Journal of Mechanical Engineering (JMechE)* 20, no. 3 (2023): 199-222. https://doi.org/10.24191/jmeche.v20i3.23908

[22] Adhikari, Pradhumna, Umesh Budhathoki, Shiva Raj Timilsina, Saurav Manandhar, and Tri Ratna Bajracharya. "A study on developing pico propeller turbine for low head micro hydropower plants in Nepal." *Journal of the Institute of Engineering* 9, no. 1 (2013): 36-53. https://doi.org/10.3126/jie.v9i1.10669

[23] Vu, Viet Luyen, Zhenmu Chen, and Young-Do Choi. "Design and performance of a pico propeller hydro turbine model." *Journal of the Korean Society of Fluid Mechanics* 21, no. 3 (2018): 44-51. https://doi.org/10.5293/kfma.2018.21.3.044